Organometallics 1990, 9, 1485-1492

Bonding Characteristics of Alkali-Metal Amides in Solution and in the Solid State: NMR and X-ray Diffraction Study of *N*-Lithioindole–*N*,*N*,*N'*,*N'*-Tetramethylethylenediamine, *N*-Sodioindole–*N*,*N*,*N'*,*N'*-Tetramethylethylenediamine, and *N*-Sodioindole–*N*,*N*,*N'*,*N''*,*N''*-Pentamethyldiethylenetriamine

Karina Gregory, Matthias Bremer, Walter Bauer, and Paul von Ragué Schleyer*

Institut für Organische Chemie, Universität Erlangen-Nürnberg, Henkestrasse 42,
D-8520 Erlangen, West Germany

Nis Peter Lorenzen, Jürgen Kopf, and Erwin Weiss*

Institut für Anorganische und Angewandte Chemie, Universität Hamburg, Martin-Luther-King-Platz 6,
D-2000 Hamburg, West Germany

Received September 27, 1989

The solid-state structures of the aromatic alkali-metal amides, *N*-lithioindole·TMEDA (1, TMEDA = *N*,*N*,*N'*,*N'*-tetramethylethylenediamine), *N*-sodioindole·TMEDA (2), and *N*-sodioindole·PMDTA (3, PMDTA = *N*,*N*,*N'*,*N''*,*N''*-pentamethyldiethylenetriamine) are compared. All these compounds are dimers with $(M-N)_2$ rings. With respect to the benzannelated anion, the Li derivative is a syn dimer (C_2 symmetry), whereas the Na amides 2 and 3 crystallize in transoid forms (C_i symmetry). Due to σ and π interactions between M and N in 1 and 2, different M-N bond lengths within the $(M-N)_2$ rings are observed. In 3 these differences disappear, and a nearly square-planar arrangement is adopted. This is due to the enhanced steric requirements of PMDTA compared to TMEDA. The nearest-neighbor relationships and aggregation of 1 also have been investigated in solution by using ^1H, ^{13}C, and $^1H-^6Li$ HOESY NMR spectroscopy. In toluene-d_8 a 3:1 equilibrium between the anti and the syn form of 1 is observed. Semiempirical molecular orbital calculations on the dimeric lithium amide indicate that there is no inherent energetic preference between the syn and anti orientations of the benzannelated anionic units.

Introduction

The aggregation of lithium and sodium amides varies impressively both in the solid state[1,2] and in solution.[3-5] The degree of association is determined largely by the nature of the anion, by the alkali-metal cations, and by the additional ligands, monodentate (e.g., diethyl ether, THF = tetrahydrofuran, HMPTA = hexamethylphosphoric triamide) or chelate (e.g., TMEDA = *N*,*N*,*N'*,*N'*-tetramethylethylenediamine, PMDTA = *N*,*N*,*N'*,*N''*,*N''*-pentamethyldiethylenetriamine). In the presence of coordinating O or N ligands, dimeric molecular complexes are favored.[1] Higher aggregates (trimers, tetramers, and polymers, e.g., $(Me_2NNa)_{10}$·4TMEDA[2b] or $(Me_2NNa)_{12}$·4TMEDA[2b])[1e,f,2] also are possible.

Central four-membered $(Li-N)_2$ rings are an important structural feature of dimeric Li amides. These usually contain tetra- or tricoordinated bridging lithium cations, as in $(PhMeNLi\cdot TMEDA)_2$[1a] and $[2,4,6\text{-}Bu(t)_3C_6H_2NHLi\cdot OEt_2]_2$.[1b] The tetragonal planar arrangement, comprised of the Li cations and the negatively charged N atoms, optimizes the electrostatic interactions (ion quadrupole model).[6]

The orientation of the organic units in an unsymmetric molecular complex depends on the size and the properties of the anion. Steric hindrance in unsymmetrical anions, e.g., in *trans*-$[Li(NHAr)(OEt_2)]_2$ (Ar = $C_6H_2Bu^t_3$-2,4,6),[1b] and the availability of intramolecular coordination sites, e.g., in $[Ph(2\text{-}py)NLi\cdot HMPTA]_2$[1c] where the pyridyl nitrogen can act as a chelating ligand, leads to transoid arrangements.

Recently, we reported the first X-ray structure of an aromatic Li amide, *N*-lithiocarbazole·2THF[1d] and solved the solid-state structure of *N*-cesiocarbazole·PMDTA.[7] Both compounds are dimers in the solid state with planar $(M-N)_2$ rings. In contrast to the other amide dimers, the carbazole moieties are tilted. In the lithium compound the cations adopt positions that suggest both "σ" and "π" interactions with the carbazole nitrogen. These π interactions are much more important in *N*-cesiocarbazole. The large coordination requirements of the cesium cation lead to the formation of a *N*-cesiocarbazole·PMDTA dimer with the cations placed above the π system of the central

---

[1] (a) Barr, D.; Clegg, W.; Mulvey, R. E.; Snaith, R.; Wright, J. *J. Chem. Soc., Chem. Commun.* **1987**, 716. (b) Cetinkaya, B.; Hitchcock, P. B.; Lappert, M. F.; Misra, M. C.; Thorne, A. J. *J. Chem. Soc., Chem. Commun.* **1984**, 148. (c) Barr, D.; Clegg, W.; Mulvey, R. E.; Snaith, J. *J. Chem. Soc., Chem. Commun.* **1984**, 700. (d) Hacker, R.; Kaufmann, E.; Schleyer, P. v. R.; Mahdi, W.; Dietrich, H. *Chem. Ber.* **1987**, *120*, 1533. (e) Lappert, M. F.; Slade, M. J.; Singh, A. *J. Am. Chem. Soc.* **1983**, *105*, 302. (f) Barr, D.; Clegg, W.; Mulvey, R. E.; Snaith, R. *J. Chem. Soc., Chem. Commun.* **1984**, 285.

[2] (a) Mootz, D.; Zinnius, A.; Böttcher, B. *Angew. Chem.* **1969**, *81*, 398. Rogers, R. D.; Atwood, J. L.; Grüning, R. *J. Organomet. Chem.* **1987**, *157*, 229. (b) Lorenzen, N. P.; Weiss, E., unpublished results.

[3] (a) Galiano-Roth, A. S.; Michaelides, E. M.; Collum, D. B. *J. Am. Chem. Soc.* **1988**, *110*, 2658. (b) Jackman, L. M.; Scarmoutzos, L. M. *J. Am. Chem. Soc.* **1987**, *109*, 5348. (c) Kallman, N.; Collum, D. B. *J. Am. Chem. Soc.* **1987**, *109*, 7466.

[4] De Pue, J. S.; Collum, D. B. *J. Am. Chem. Soc.* **1988**, *110*, 5518, 5524. Jackman, L. M.; Scarmoutzos, L. M.; Smith, D. B.; Williard, P. G. *J. Am. Chem. Soc.* **1988**, *110*, 6058.

[5] Reed, D.; Barr, D.; Mulvey, R. E.; Snaith, R. *J. Chem. Soc., Dalton Trans.* **1986**, 557. Kimura, B. Y.; Brown, T. L. *J. Organomet. Chem.* **1971**, *26*, 57.

[6] Streitwieser, A., Jr. *Acc. Chem. Res.* **1984**, *17*, 353. Kaufmann, E.; Clark, T.; Schleyer, P. v. R. *J. Am. Chem. Soc.* **1984**, *106*, 1856.

[7] Gregory, K.; Bremer, M.; Schleyer, P. v. R.; Klusener, P. A. A.; Brandsma, L. *Angew. Chem.* **1989**, *101*, 1261; *Angew. Chem., Int. Ed. Engl.* **1989**, *28*, 1224.

0276-7333/90/2309-1485$02.50/0

Table I. Selected Bond Lengths (Å) and Angles (deg) in M–indole•L (M = Li, Na; L = TMEDA, PMDTA)

	M = Li, L = TMEDA (1)	M = Na, L = TMEDA (2)	M = Na, L = PMDTA (3)
	Bond Lengths		
M–N(1)	2.231 (10)	2.478 (5)	2.474 (4)
M–N(1a)	2.004 (7)	2.356 (5)	2.481 (5)
M–C(2)	2.757 (11)	2.967 (7)	3.386 (6)
M–C(9)	2.962	2.994 (6)	3.230 (5)
M–N(2)	2.233 (7)	2.433 (5)	2.623 (5)
M–N(3)	2.156 (6)	2.474 (5)	2.559 (4)
M–N(4)			2.608 (5)
M–H(2)	3.100	3.295	
M–H(7)	3.215	3.667	
M–M(1a)	2.799 (11)	3.331 (5)	3.501 (5)
	Bond Angles		
N(1)–M–N(2)	120.6 (4)	121.9 (2)	99.1 (1)
N(1)–M–N(3)	119.1 (4)	128.9 (2)	168.8 (10)
N(1)–M–N(4)			108.3 (1)
N(2)–M–N(3)	84.9 (2)	76.7 (2)	71.2 (1)
N(2)–M–N(4)			110.4 (1)
N(1)–M–N(1a)	96.6 (3)	92.9 (2)	90.1 (2)
C(2)–N(1)–M	96.8 (3)	96.5 (2)	121.2 (2)
C(9)–N(1)–M	108.7 (3)	97.8 (2)	110.6 (2)
M(a)–N(1)–M	82.5 (3)	87.1 (2)	89.9 (1)
C(2)–N(1)–M(a)	125.0 (3)	131.4 (2)	129.9 (2)
C(9)–N(1)–M(a)	128.2 (3)	124.7 (2)	99.4 (2)

Table II. Fractional Coordinates and Anisotropic Thermal Parameters (U_{eq}) for [M–Indole•TMEDA]$_2$ {(M = Li (1), M = Na (2)} and [Na–indole•PMDTA]$_2$ (3) ($U_{eq} = {}^1/_3(U_{11} + U_{22} + U_{33})$)

atom	*X/a*	*Y/b*	*Z/c*	*U*(eq), Å^2
		M = Li (1)		
C(23A)	0.1231 (5)	0.2714 (11)	1.0294 (6)	0.056 (3)
C(23B)	0.1563 (4)	0.2474 (9)	1.0090 (5)	0.063 (3)
Li	0.0482 (3)	0.3909 (8)	0.8462 (4)	0.038 (4)
N(1)	0.0558 (2)	0.4121 (4)	0.7241 (2)	0.039 (2)
C(2)	0.1017 (2)	0.2928 (5)	0.7469 (3)	0.044 (3)
C(3)	0.1665 (2)	0.3384 (5)	0.7711 (3)	0.044 (3)
C(8)	0.1639 (2)	0.5002 (5)	0.7650 (2)	0.035 (2)
C(4)	0.2117 (2)	0.6157 (6)	0.7832 (3)	0.051 (3)
C(5)	0.1908 (3)	0.7649 (6)	0.7710 (3)	0.061 (3)
C(6)	0.1223 (3)	0.8050 (6)	0.7404 (3)	0.061 (3)
C(7)	0.0733 (2)	0.6933 (5)	0.7230 (3)	0.049 (3)
C(9)	0.0938 (2)	0.5403 (5)	0.7350 (3)	0.033 (2)
N(2)	0.0894 (2)	0.1832 (4)	0.9369 (2)	0.042 (2)
N(3)	0.1208 (2)	0.5156 (4)	0.9711 (2)	0.040 (2)
C(32)	0.1730 (2)	0.6001 (6)	0.9652 (3)	0.083 (3)
C(31)	0.0872 (2)	0.6204 (6)	1.0001 (3)	0.086 (4)
C(33)	0.1564 (3)	0.3984 (5)	1.0430 (3)	0.082 (3)
C(21)	0.1174 (3)	0.0582 (7)	0.9132 (4)	0.157 (7)
C(22)	0.0392 (3)	0.1142 (7)	0.9488 (4)	0.135 (5)
		M = Na (2)		
Na	0.4377 (1)	0.1012 (1)	0.1084 (1)	0.0746 (4)
N(1)	0.4721 (3)	0.8152 (3)	0.1204 (2)	0.084 (1)
C(2)	0.5538 (5)	0.7534 (4)	0.2249 (4)	0.101 (2)
C(3)	0.4588 (7)	0.6935 (5)	0.3418 (4)	0.111 (2)
C(4)	0.1580 (6)	0.6771 (5)	0.3923 (4)	0.126 (2)
C(5)	0.0281 (6)	0.7198 (5)	0.3277 (5)	0.146 (3)
C(6)	0.0397 (6)	0.7955 (5)	0.1930 (5)	0.126 (2)
C(7)	0.1839 (5)	0.8290 (4)	0.1194 (4)	0.096 (2)
C(8)	0.3048 (5)	0.7140 (3)	0.3153 (3)	0.088 (1)
C(9)	0.3190 (4)	0.7893 (3)	0.1790 (3)	0.071 (1)
N(2)	0.1975 (3)	0.2319 (3)	0.2178 (2)	0.073 (1)
N(3)	0.5417 (3)	0.2193 (3)	0.2358 (2)	0.072 (1)
C(21)	0.1132 (5)	0.1152 (4)	0.3247 (4)	0.104 (2)
C(22)	0.0885 (6)	0.3298 (6)	0.1269 (5)	0.141 (2)
C(23)	0.2519 (4)	0.3428 (4)	0.2663 (4)	0.102 (2)
C(31)	0.6121 (5)	0.3613 (5)	0.1584 (4)	0.113 (2)
C(32)	0.6584 (5)	0.1029 (5)	0.3141 (4)	0.120 (2)
C(33)	0.3982 (3)	0.2577 (5)	0.3329 (3)	0.102 (2)
		M = Na (3)		
Na	0.0470 (1)	0.1231 (1)	0.3756 (1)	0.0320 (3)
N(1)	0.0240 (3)	0.0970 (2)	0.6049 (2)	0.0369 (6)
C(2)	0.1330 (3)	0.1221 (3)	0.6440 (3)	0.0397 (8)
C(3)	0.0637 (4)	0.2221 (3)	0.7393 (3)	0.0426 (8)
C(4)	−0.1051 (3)	0.2657 (3)	0.7644 (2)	0.0378 (7)
C(5)	−0.2467 (4)	0.3389 (3)	0.8512 (3)	0.0502 (9)
C(6)	−0.3961 (4)	0.3684 (3)	0.8514 (3)	0.0553 (9)
C(7)	−0.4136 (4)	0.2901 (3)	0.7686 (3)	0.0496 (9)
C(8)	−0.2772 (3)	0.1966 (3)	0.6816 (3)	0.0403 (8)
C(9)	−0.1243 (3)	0.1862 (3)	0.6800 (2)	0.0338 (7)
N(2)	0.3375 (3)	0.1479 (2)	0.2731 (2)	0.0368 (6)
N(3)	0.1061 (2)	0.1792 (2)	0.1345 (2)	0.0337 (6)
N(4)	−0.1711 (3)	0.3606 (2)	0.3459 (2)	0.0380 (6)
C(20)	0.2943 (5)	0.2921 (3)	0.3159 (4)	0.0519 (1)
C(21)	0.4767 (3)	0.0555 (4)	0.3089 (3)	0.0459 (9)
C(22)	0.3843 (3)	0.1424 (3)	0.1328 (3)	0.0416 (8)
C(30)	0.2496 (3)	0.2261 (3)	0.0816 (3)	0.0403 (8)
C(31)	0.1378 (4)	0.0484 (3)	0.0714 (3)	0.0426 (8)
C(32)	−0.0355 (3)	0.2905 (3)	0.1152 (3)	0.0402 (8)
C(40)	−0.2112 (4)	0.4734 (3)	0.4318 (3)	0.0493 (9)
C(41)	−0.31262 (4)	0.3216 (4)	0.3681 (3)	0.0526 (1)
C(42)	−0.1099 (3)	0.4092 (3)	0.2113 (3)	0.0424 (8)

five-membered ring. This leads to Cs–C separations of 3.23–3.75 Å. Similar structural features may be expected for smaller cations (Li^+, Na^+) when the electronic properties of the amide anion are altered, e.g., when charge delocalization in the aromatic system is reduced, as in the singly benzannelated indolyl system.

Two types of dimers of the metalated species are possible, with syn or anti orientation of the benzannelated rings. Only limited structural information is available on aromatic Na amides.[8] Na and Li organic compounds often possess similar geometries, but many exceptions are known.[9] Due to the larger Na–X distances (which decrease the association energy) and the increased coordination requirements of the larger Na^+, sodium compounds often form smaller aggregates in the presence of an excess of a Lewis base (e.g., BuLi is a tetramer and BuNa is a monomer in THF).[10,11] However, the larger coordination sphere of the Na^+ ion can also favor an increased number of metal–anion contacts, e.g., CpNa·TMEDA[12] and $C_5H_4CMeONa\cdot THF$[13] are polymers, whereas $C_5H_4SiMe_3Li$[14] is monomeric in the solid state.

We have now examined both the cation (Li^+, Na^+) influence and that of different polydentate ligands (TMEDA and PMDTA) on the structures of unsymmetric aromatic metal amides in the solid state and in solution. We compare the crystal structures of two differently solvated aromatic Na amides with that of an analogous Li compound. The temperature dependence of the chemical shifts of the TMEDA solvates in solution has been examined by ^1H and ^{13}C NMR spectroscopy. Two-dimensional ^1H–^6Li HOESY NMR confirms the existence of agostic Li–H interactions in the Li compound predicted by MNDO calculations.

Results and Discussion

X-ray Structure of *N*-Lithioindole·TMEDA (1). Direct metalation of indole with *n*-BuLi in a 1:1 mixture of hexane and benzene in the presence of 1 equiv of TMEDA yielded colorless crystals of X-ray quality after a few days at 0 °C. The structure was solved by direct

---

[8] Gregory, K.; Bremer, M.; Schleyer, P. v. R. Unpublished results.

[9] Schade, C.; Schleyer, P. v. R. *Adv. Organomet. Chem.* **1988**, *27*, 169.

[10] McGarrity, J. F.; Ogle, C. A. *J. Am. Chem. Soc.* **1985**, *107*, 1805. Seebach, D.; Hässig, R.; Gabriel, J. *Helv. Chim. Acta* **1983**, *66*, 308.

[11] Schade, C.; Bauer, W.; Schleyer, P. v. R. *J. Organomet. Chem.* **1985**, *295*, C25.

[12] Ayoagi, T.; Shearer, H. M. M.; Wade, K.; Whitehead, G. *J. Organomet. Chem.* **1979**, *175*, 21.

[13] Rogers, R. D.; Atwood, J. L.; Rausch, M. D.; Macomber, D. W.; Hart, W. P. *J. Organomet. Chem.* **1982**, *238*, 79.

[14] Lappert, M. F.; Singh, A.; Engelhardt, L. M.; White, A. H. *J. Organomet. Chem.* **1984**, *262*, 271.

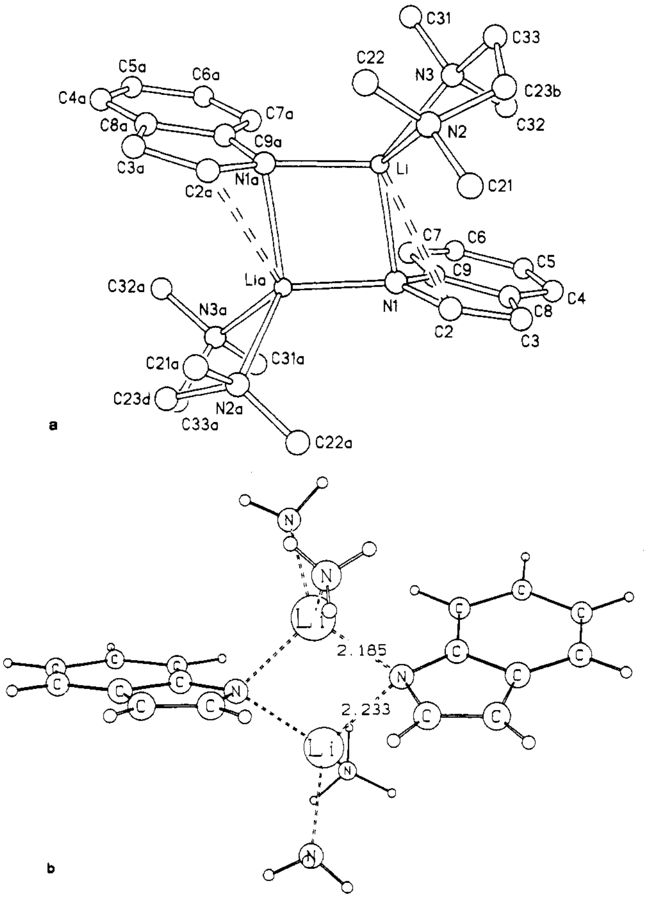

Figure 1. (a) Molecular structure of *N*-lithioindole·TMEDA (1); (b) MNDO optimized structure of *syn*-(*N*-lithioindole·2NH$_3$)$_2$.

methods. In the solid state, 1 is a dimer with tetracoordinate anion bridging lithium cations. The benzene rings are oriented toward the same side of the aggregate resulting in C_2 symmetry (Figure 1a). Table I gives geometrical information, and Table II contains fractional coordinates and anisotropic temperature factors.

The two cations adopt different positions in the dimer. Li(a) is in the plane of the indole system and exhibits a strong σ-interaction with N(1) (2.00 Å). The symmetry-related cation Li is positioned above the nitrogen. Hence, dimerisation leads to π-coordination of the σ-bonded lithium with the p_z orbital of the nitrogen in the second anion. This π-interaction gives a 2.23-Å N(1)–Li distance. The coordination sphere of the lithiums, when the nitrogen centers of the chelating TMEDA ligand are taken into account, is distorted tetrahedral.

The (Li–N)$_2$ ring is not planar. Both cations are bent away from the benzene rings toward the α-carbon atoms C(2) and C(2a) in the five-membered ring. This bending is due to interaction of the lithium cations with the π system of the pyrrole moiety. Presumably, the relative weakness of the Li–N(1) π interaction results in a relatively short Li(a)–C(2) distance of 2.76 Å. Due to charge delocalization into the annelated benzene rings of *N*-lithiocarbazole·2THF, only the bonding to nitrogen (the atom with the highest charge density) is favored. In the *N*-lithioindole dimer the main interaction also takes place between the Li cation and the nitrogen; however, the cations bend toward the enaminic moiety, where the π-electron density should be higher than that in the opposite direction. The formal pentacoordination of Li$^+$ is unusual for Li amides.

X-ray Structure of *N*-Sodioindole·TMEDA (2). *N*-sodioindole·TMEDA was prepared in two ways: by

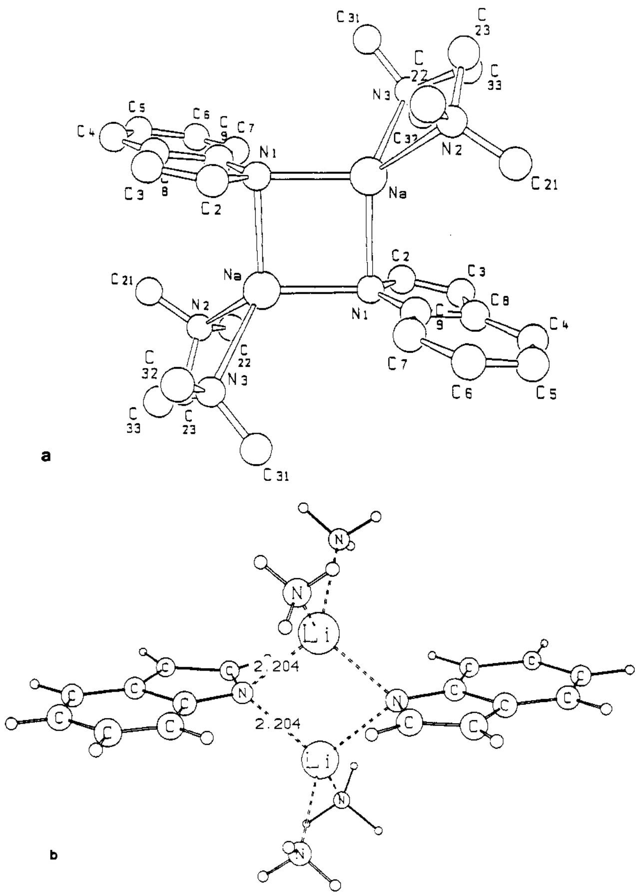

Figure 2. (a) Molecular structure of *N*-sodioindole·TMEDA (2); (b) MNDO optimized structure of *anti*-(*N*-lithioindole·2NH$_3$)$_2$.

metalation of indole with *n*-butylsodium and by metal–metal exchange[15] of lithioindole·TMEDA with sodium *tert*-amylate. After 2 days at 0 °C colorless crystals of 2 were obtained. The preparation and structure determination of 2 are described in the experimental part. The structural features of 2 are similar to those of 1, with regard to the degree of aggregation and coordination. As shown in Figure 2a, 2 also exists as a dimer in the solid state with bridging sodium cations. Each Na cation is complexed by one TMEDA ligand. Table I compares the geometry with that of the Li compound. Table II gives the fractional coordinates and the anisotropic temperature factors.

Surprisingly the organic moieties are orientated *anti*: the transoid dimer has molecular C_i symmetry. The (Na–N)$_2$ ring is planar with Na–N bond lengths of 2.36 Å for the σ bond and 2.48 Å for the π-interaction.

As Figure 2a shows, the σ- and π-interactions of the sodium cations with the indole anions are enhanced. The angles in the four membered Na–N–Na–N ring are closer to 90° (the angle between the nitrogen p_z and sp^2 orbitals) than in 1. The difference between the Na–N σ- and π-bond lengths, only 0.12 Å, is less than the 0.23-Å difference in the Li compound. Hence, both Na–N interactions are nearly equivalent, whereas the Li–N π-interaction must be weaker than the σ-bond. In the sodium compound, the cation is more centrally placed above the nitrogen. This satisfies the increased coordination requirements of Na$^+$ by interacting with both α-carbon atoms within one anionic moiety. The Na cations in 2 are six-coordinated. The Na(1)–C(2) and Na(1)–C(9) distances, 2.97 and 2.99 Å, respectively, are within the range of the largest Na–C

---

[15] Lochmann, L.; Trekoval, J. *Coll. Czech. Chem. Commun.* **1988**, *53*, 76.

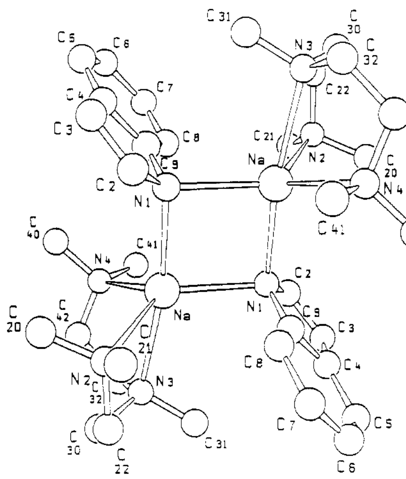

Figure 3. Molecular structure of *N*-sodioindole·PMDTA (**3**).

contacts in the sodio-cyclopentadiene derivatives.[12,13] These distances are in good agreement with ab initio calculations by Mulvey and co-workers on monomeric uncomplexed Na-aza-allyl arrangements,[16] where the computed Na–N and Na–C distances are 2.307 and 2.538 Å, respectively.

X-ray Structure of *N*-Sodioindole·PMDTA (3). The tridentate pentamethyldiethylenetriamine (PMDTA) ligand may reduce the degree of oligomerization of organoalkali-metal compounds. Examples are the formation of monomeric lithiophenyl·PMDTA[17] in contrast to the (lithiophenyl·TMEDA)$_2$ dimer.[18] In both cases, Li displays its common four coordination. The increased ionic radius of Na favors a higher coordination number. This is shown by the formation of (sodiophenyl·PMDTA)$_2$[19] dimer, in contrast to monomeric lithiophenyl·PMDTA. Do the TMEDA and PMDTA solvates of sodioindole differ?

The preparation of *N*-sodioindole·PMDTA was similar to that of its TMEDA analogue. The X-ray structure of **3** revealed a dimer with similar features as **2**, i.e., a centrosymmetric arrangement with transoid orientation of the indolyl groups. The main difference is the inclination of the indolyl groups with respect to the (Na–N)$_2$ ring, as shown in Figure 3. The indolyl groups in **3** adopt a more symmetrical orientation. The difference between the σ and π interactions disappears. The Na–N bond lengths (Table I) become essentially identical (2.47 and 2.48 Å) and the angles formed between the indolyl planes and the adjacent N–Na bonds are very similar (132.0 and 129.0°). Hence, the (Na–N)$_2$ ring is an almost perfect square (N–Na–N 90.1°, Na–N–Na (89.9°). Obviously the difference in the structure of **3** compared to **2** is due to the greater steric requirements of PMDTA compared to TMEDA. There seems to be only a small difference in energy between both structural types. Thus, the enhanced repulsion between the indolyl anion and the PMDTA ligands produces a more symmetrical ring arrangement. In the PMDTA complex **3**, the pentacoordinate Na$^+$ cations display a distorted trigonal-bipyramidal arrangement. The atoms N(2), N(4), and N(1′) occupy the equatorial, N(1) and N(3) the axial positions.

Calculations on Solvated *N*-Lithioindoles. Semiempirical calculations (MNDO)[20] are useful in reproducing and even in predicting the general structural features of organolithium compounds[21-23] in general and of lithium amides[1d] in particular (e.g., dilithiated 2,6-trimethyl(silylmethyl)pyridine·TMEDA,[21] [3,6-bis(lithio·THF)-2,2,7,7-tetramethyl-3,4,5-octatriene]$_2$,[22] 1,3-dilithiodibenzyl ketone·TMEDA[23] and (*N*-lithiocarbazole·2THF)$_2$.[1d] MNDO calculations on the lithioindole-2NH$_3$ dimer (the NH$_3$ groups serve as a model for the chelating ligand TMEDA) show that there is only very little energetic preference of the anti over the syn isomer ($\Delta\Delta H_f° = -0.3$ kcal/mol). Hence, whatever effect determines the arrangement of the organic moieties in the solid is not relevant in the gas phase. The calculated structures are in good agreement with the crystal structures. Although slightly underestimated, the difference in the σ- and the π-interactions between the lithium cations and the indole nitrogen were calculated with reasonable accuracy. Figures 1b and 2b compare the MNDO and the solid-state dimer structures.

Table III. ^{13}C NMR Chemical Shifts of Lithioindole•TMEDA[a]

	−81 °C		−91 °C	
	anti	syn	anti	syn
C(2)	136.99	136.69	137.01	136.69
C(3)	101.75	101.75	101.72	101.72
C(4)	120.45	120.45	120.43	120.43
C(5)[b]	117.03	117.03	116.99	116.99
C(6)[b]	118.16	118.34	118.16	118.32
C(7)	114.79	115.33	114.77	115.32
C(8)	148.85	149.03	148.83	149.02
C(9)	132.62	132.62	132.56	132.56
TMEDA CH$_3$[c]	46.18		46.16	
TMEDA CH$_3$[d]	48.06 41.17		*e*	
TMEDA CH$_2$[c]	58.25		58.20	
TMEDA CH$_2$[d]	56.11		*e*	

[a] Crystals of TMEDA-containing dimer, dissolved in toluene-d_8. [b] Assignments may be interchanged. [c] "Free" TMEDA from small amounts of hydrolysis products; see Figure 5 and text. [d] Lithium-bound TMEDA; see Figure 5 and text. [e] Split into several lines; see Figure 5 and text.

Table IV. ^{1}H NMR Chemical Shifts of Lithioindole•TMEDA[a] (1) at −81 °C

	anti	syn		anti	syn
H(2)	7.69	7.56	H(5)	7.38	7.38
H(3)	7.09	7.09	H(6)	7.40	7.44
H(4)	8.15	8.15	H(7)	7.69	7.84

[a] Crystals of TMEDA containing dimer dissolved in toluene-d_8.

NMR Results. According to the MNDO calculations the syn and anti isomers of the lithioindole dimer have nearly the same energy. However, in the solid state **1** (C_2 symmetry) has the syn conformation, while **2** and **3** are anti isomers with C_i symmetry. To obtain more information about the effects responsible for these differences, **1** and **2** were examined in solvents of low and high polarity by NMR spectroscopy at various temperatures. In nonpolar, noncoordinating solvents, it should be possible to observe dimeric aggregates containing the TMEDA ligand.

Both the ^{13}C and ^{1}H NMR spectra (Tables III and IV, respectively) of **1** in toluene-d_8 (saturated solution) at −80 °C show two sets of signals for the indole moiety with

---

(16) Andrews, P. C.; Armstrong, D. R.; Mulvey, R. E. *J. Am. Chem. Soc.* **1988**, *110*, 5235.

(17) Schümann, U.; Kopf, J.; Weiss, E. *Angew. Chem., Int. Ed. Engl.* **1985**, *24*, 215.

(18) Thönnes, D.; Weiss, E. *Chem. Ber.* **1978**, *111*, 3157.

(19) Schümann, U.; Behrens, U.; Weiss, E. *Angew. Chem., Int. Ed. Engl.* **1989**, *28*, 476.

(20) Dewar, M. J. S.; Thiel, W. *J. Am. Chem. Soc.* **1977**, *99*, 4899, 4907.

(21) Hacker, R.; Schleyer, P. v. R.; Reber, G.; Müller, G.; Brandsma, L. *J. Organomet. Chem.* **1986**, *316*, C4.

(22) Neugebauer, W.; Geiger, G. A. P.; Kos, A. J.; Stezowski, J. J.; Schleyer, P. v. R. *Chem. Ber.* **1985**, *118*, 1504.

(23) Kos, A. J.; Clark, T.; Schleyer, P. v. R. *Angew. Chem., Int. Ed. Engl.* **1984**, *23*, 620. Dietrich, H.; Mahdi, W.; Wilhelm, D.; Clark, T.; Schleyer, P. v. R. *Angew. Chem., Int. Ed. Engl.* **1984**, *23*, 620.

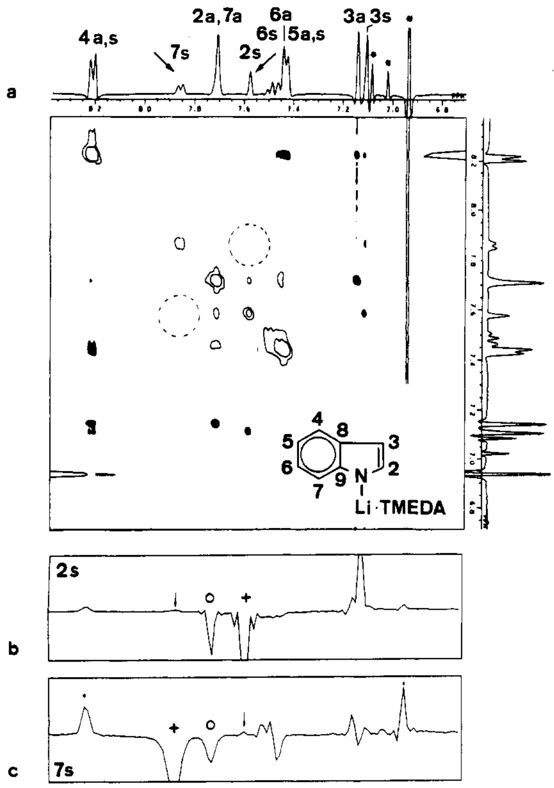

Figure 4. (a) 2D ROESY contour plot of 1 in toluene-d_8 at −91 °C (saturated solution). Negative contours are due to NOE and are filled. Dotted circles represent NOEs expected from a reversed syn/anti assignment (see text). For numbering, see formulas in text. s = syn, a = anti isomer; for details, see experimental section; * = solvent signal (toluene-d_8) (b) and (c) f_1 traces [H(2)s and H(7)s, respectively; indicated by arrows in Figure 4a] of the ROESY plot (Figure 4a). The arrows indicate positions of expected NOEs in case of reversed syn/anti assignment (see text). Peaks marked with asterisks are due to NOEs to the CH_3 groups of TMEDA and are folded in; + = diagonal peak; O = exchange cross peak.

Chart I

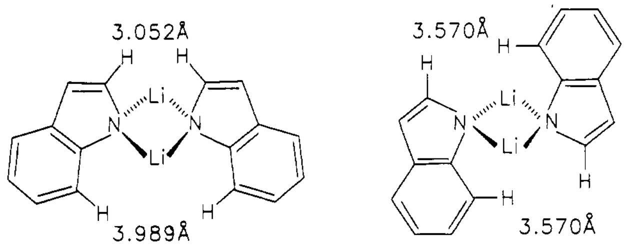

different intensities (3:1 molar ratio). Due to the similarity of the ^{13}C chemical shifts, we conclude that these spectra reflect the same state of aggregation and are due to the anti and the syn dimer.

The proton and carbon resonance assignments within each signal set were determined easily by using 2D NMR (COSY, C–H shift correlation). However, the assignment of the syn and anti species proved to be less trivial. For this purpose we employed rotating frame nuclear Overhauser spectroscopy (ROESY).[24] Compared to the conventional 2D NOESY method,[24] ROESY offers the advantage that even at low temperatures cross peaks due to chemical exchange are antiphase to NOE cross peaks (resulting from dipolar relaxation due to spatial proximity). Chart I shows both the syn and the anti dimer of lithioindole with the MNDO distances of the nearest hydrogen contacts between the monomer subunits. Due to isochronicity of the proximal hydrogen atoms, no NOE cross peak should be observed in the syn isomer. In contrast, a moderate NOE can be expected between H(2) and H(7) for the anti isomer. Figure 4 shows the 2D ROESY spectrum of lithioindole in toluene-d_8, obtained at −90 °C. Clearly, no NOE cross peak between H(2) and H(7) of the minor isomer is observable, neither in the contour plot (Figure 4a) nor in the f_1 traces of H2 and H7 (Figure 4b,c). This suggests strongly that the minor species is the syn isomer. Unfortunately, the H(2) and H(7) proton resonances of the major isomer coincide, thus precluding the observation of the expected NOEs.

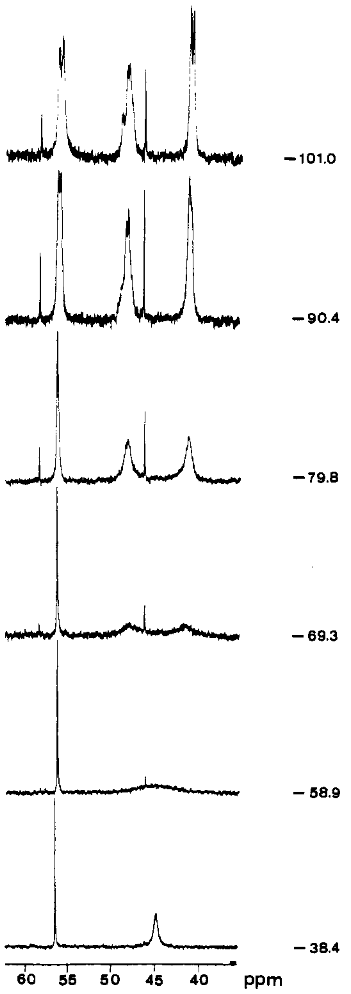

Figure 5. ^{13}C signals of TMEDA of 1 at various temperatures (°C). Crystals of 1 dissolved in toluene-d_8, saturated solution.

However, another spectral feature confirms the assignment of the syn and the anti species. The ^1H resonance of H(7) of the minor species appears downfield from the corresponding signal of the major species. This downfield shift is compatible with the syn isomer, in which both H(7) protons experience the ring current of their neighboring benzene ring. Likewise, H(2) of the minor species is upfield from H(2) of the major species: in the syn isomer H(2) experiences no downfield shift due to a neighboring aromatic ring. Hence, we believe that a 3:1 anti/syn lithioindole dimer ratio is present under these conditions.

The TMEDA signals in the ^{13}C NMR spectra of lithioindole in toluene-d_8 (prepared by dissolving crystals containing 1 equiv of TMEDA) show strong variation with the temperature (Figure 5). At −40 °C, only one signal for the CH_3 and for the CH_2 groups is present. Upon cooling,

---

[24] Kessler, H.; Gehrke, M.; Griesinger, C. *Angew. Chem., Int. Ed. Engl.* **1988**, *27*, 490.

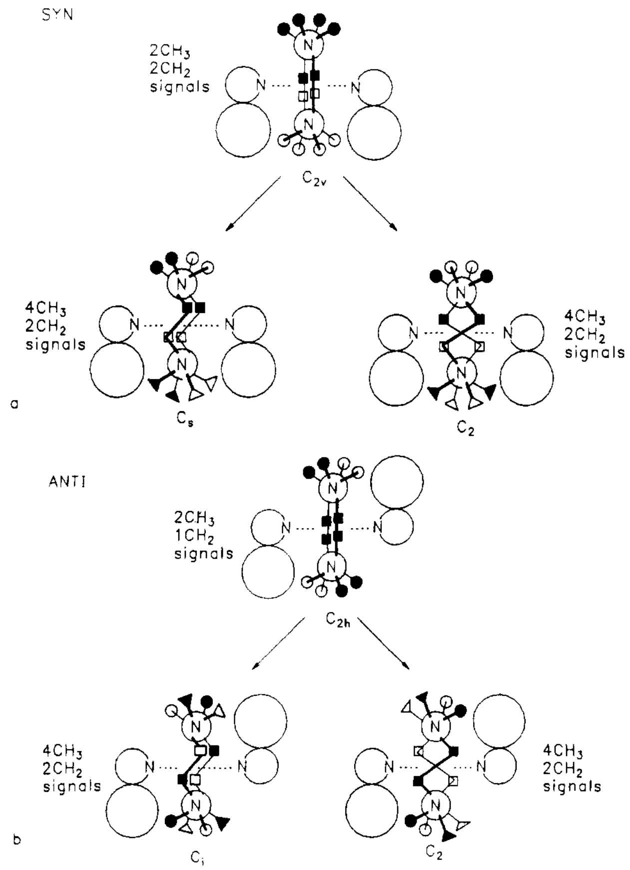

Figure 6. Lithioindole dimers, schematic representation (side view with symbolized indole rings); TMEDA conformations in time averaged (top row) and in fixed conformations (bottom row) to account for the ^{13}C NMR spectral observations of Figure 5. Identical symbols (filled or open circles, squares, triangles) indicate isochronous groups (homotopic or enantiotopic), differing symbols denote diastereotopic groups.

the CH_3 signal splits into two broad lines whereas the CH_2 resonance gradually broadens. At the lowest accessible temperature further splitting occurs to give a total of six distinct resonance lines. In addition, at all temperatures, two sharp lines are observed at 46.2 and 58.2 ppm. These must be due to "free" TMEDA (the product of small amounts of hydrolysis) which is not bound to lithium and which is obviously not involved in the dynamic process. Tentatively, we interpret these observations as follows. There is relatively slow chemical exchange between the syn and the anti isomer. This is indicated, e.g., by distinct signals for C(7)(syn) and C(7)(anti) at -70 °C ($\Delta\nu$ = 52 Hz). However, within a syn or an anti aggregate, reorientation of TMEDA is faster (coalescence of the CH_3 signals at ca. -65 °C, $\Delta\nu$ = 693 Hz). This must proceed via cleavage of one chelate Li-N bond, a "180° turn" of η^1-bound TMEDA, and return of the uncomplexed nitrogen atom to lithium. Due to the observation of separate sharp signals for free TMEDA, complete detachment of TMEDA from lithium can be ruled out. The additional splitting observed at temperatures below -90 °C might be explained by conformations of TMEDA "frozen" on the NMR time scale. This is depicted in Figure 6. On cooling, the "time averaged" C_{2v} conformation of the syn dimer and the C_{2h} conformation of the anti dimer are transformed into the C_2 and C_s (syn) and C_2 and C_i (anti) energy minima, respectively. Assuming equal populations, a total of 16 distinct signals for the CH_3 groups and 8 signals for the CH_2 groups can be expected. Due to overlap and/or coalescence and/or unequal population of the conformers, only some of these lines are resolved in Figure 5, top spectrum. Similar studies have been carried out on lithium isopropylcyclohexylamide/THF,[3a] on lithium indoline/ether,[3b] and on lithiated cyclohexanone phenylimine/THF.[3c] The results are in agreement with our findings: approximate 1/1 equilibria between syn and anti isomers are present in solution.

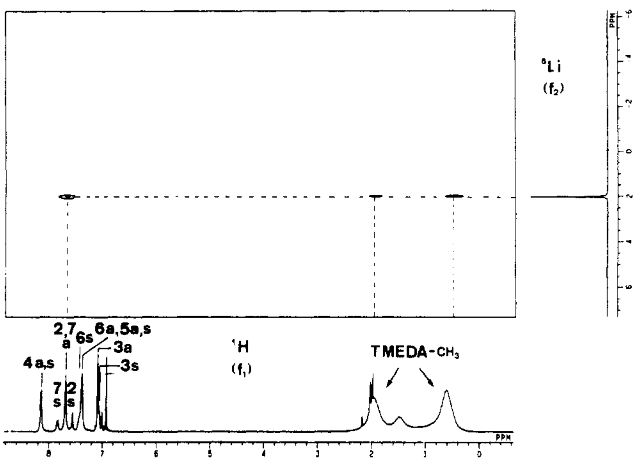

Figure 7. 2D ^{6}Li-^{1}H HOESY; crystals of ([^{6}Li]lithioindole·TMEDA)$_2$ dissolved in toluene-d_8, -81 °C, saturated solution, mixing time, 1.8 s. For numbering and assignments, see Figure 4 and text.

Table V. ^{13}C NMR Chemical Shifts of Sodioindole•TMEDA[a] at 26 °C

atom	δ, ppm	atom	δ, ppm
C(2)	137.13	C(6)[b]	118.32
C(3)	100.61	C(7)	114.26
C(4)	120.40	C(8)	147.59
C(5)[b]	116.94	C(9)	132.24

[a] Crystals of TMEDA-containing dimer dissolved in toluene-d_8. [b] Assignments may be interchanged.

Table VI. ^{1}H NMR Chemical Shifts of Sodioindole•TMEDA[a] (2) at 26 °C

atom	δ, ppm	atom	δ, ppm
H(2)	7.84	H(5)	7.08
H(3)	6.92	H(6)	7.14
H(4)	7.62	H(7)	7.68

[a] Crystals of TMEDA-containing dimer dissolved in toluene-d_8.

The MNDO calculations also predict relatively short Li-H(2) separations of ~3 Å in the dimer of 1. These distances are within the range of Li-H contacts (agostic interactions)[25] observable by two-dimensional heteronuclear Overhauser effect spectroscopy[26] (^{6}Li-^{1}H 2D HOESY).[27-33] This method was introduced by our group and successfully demonstrated in the investigation of short lithium-hydrogen distances.[27-33] The NMR data from

---

(25) Brookhart, M.; Green, M. L. H. *J. Organomet. Chem.* **1983**, *250*, 395. Koga, N.; Obara, S.; Morokuma, K. J. *J. Am. Chem. Soc.* **1984**, *106*, 4625. Erker, G.; Frömberg, W.; Angermund, K.; Schlund, R.; Krüger, C. *J. Chem. Soc., Chem. Commun.* **1986**, 372.

(26) Benn, R.; Günther, H. *Angew. Chem., Int. Ed. Engl.* **1983**, *22*, 390.

(27) Bauer,. W.; Müller, G.; Pi, R.; Schleyer, P. v. R. *Angew. Chem., Int. Ed. Engl.* **1986**, *25*, 1103.

(28) Bauer, W.; Clark, T.; Schleyer, P. v. R. *J. Am. Chem. Soc.* **1987**, *109*, 970.

(29) Bauer, W.; Feigel, M.; Müller, G.; Schleyer, P. v. R. *J. Am. Chem. Soc.* **1988**, *110*, 6033.

(30) Bauer, W.; Schleyer, P. v. R. *J. Am. Chem. Soc.* **1989**, *111*, 7191.

(31) Bauer, W.; Winchester, W. R.; Schleyer, P. v. R. *Organometallics* **1987**, *6*, 2371.

(32) Bauer, W.; Klusener, P. A. A.; Harder, S.; Kanters, J. A.; Duisenberg, A. J. M.; Brandsma, L.; Schleyer, P. v. R. *Organometallics* **1988**, *7*, 552.

Table VII. Summary of Crystallographic Data for Lithio- and Sodioindole•TMEDA and Sodioindole•PMDTA

	1	2	3
empirical formula	$C_{28}H_{44}N_6Li_2$	$C_{28}H_{44}N_6Na_2$	$C_{34}H_{58}N_8Na_2$
color, habit	colorless columns	colorless columns	colorless columns
crystal size, mm	0.5 × 0.5 × 0.3	0.4 × 0.4 × 0.8	0.3 × 0.5 × 0.6
crystal system	monoclinic	triclinic	triclinic
space group	$C2/c$	$P\bar{1}$	$P\bar{1}$
unit cell			
a, Å	23.080 (12)	8.744 (6)	9.393 (12)
b, Å	8.711 (4)	8.986 (16)	10.032 (11)
c, Å	17.363 (9)	11.008 (8)	11.189 (17)
α, deg		69.60 (13)	81.3 (1)
β, deg	123.84 (3)	76.48 (6)	68.1 (1)
γ, deg		76.84 (11)	69.3 (1)
vol, Å^3	2899 (3)	778 (2)	915 (2)
Z	4	1	1
ρ_x, g cm^{-3}	1.10	1.09	1.134
μ, mm^{-1}	0.61	0.73	0.71
$F(000)$	1040	276	340
diffractometer	Nicolet R3mV	Enraf-Nonius CAD4	Enraf-Nonius CAD4
radiation	Mo Kα (λ = 0.71073 Å)	Cu Kα (λ = 1.54051 Å)	Cu Kα (λ = 1.54051 Å)
temp, K	200	293	173
monochromator	highly oriented graphite crystal		
2θ range, deg	4–60	4.5–120	4.5–153
scan type	ω	$\theta/2\theta$	$\theta/2\theta$
scan range	1.6 (ω)	1.6 (2θ)	1.6 (2θ)
scan speed[a]	variable	variable	variable
std reflns	3 measd every 100 reflns	3 measd every 2 h	
indep reflns	4241	3386	4172
obsd reflns	2163, $F > 6\sigma(F)$	1850, $F > 4\sigma(F)$	3389, $F > 5\sigma(F)$
solution	direct methods (SHELXTL PLUS) and SHELXS-86		
refinement	full-matrix least-squares		
quantity minimized	$\sum w(F_o - F_c)^2$		
hydrogen atoms	riding model, isotropic U		
weighting scheme	$w^{-1} = \sigma^2(F) + 0.0F^2$		
R	0.099	0.059	0.085
R_w	0.075	0.048	0.093
data/parameter	12.9/1	10.0/1	10.7/1

[a] 3–15°/min in ω.

[^{6}Li]lithioindole·TMEDA confirmed the theoretical prediction. The ^{6}Li,^{1}H HOESY spectrum at −81 °C in toluene-d_8 is shown in Figure 7. Only one ^{6}Li signal of 1 is found, indicating identical ^{6}Li shifts and/or coalescence of the ^{6}Li signals of the syn and the anti dimer. The upfield cross peaks at $\delta_{^1H}$ 0.52 and 1.93 ppm are due to interactions between the lithium cations and the TMEDA N-methyl hydrogens. The cross peak at 7.69 ppm, corresponding to both H(2) and H(7) of the anti dimer, shows spatial interaction of these protons with the lithium cation, in agreement with the MNDO structure. However, no Li–H interactions can be seen in the syn dimer, presumably due to its much lower concentration.

To obtain information about the structure of N-sodioindole·TMEDA in toluene-d_8 solution, we recorded ^{13}C and ^{1}H spectra under the same conditions used for 1. The ^{13}C and ^{1}H NMR chemical shifts of 2 in toluene-d_8 solution are given in Tables V and VI. By comparison with the NMR data of 1, 2 should be a dimer. From the line widths of the signals, we conclude that the TMEDA ligands are coordinated to sodium. However, due to decreasing solubility with decreasing temperature, the syn and anti orientations cannot be assigned unambiguously.

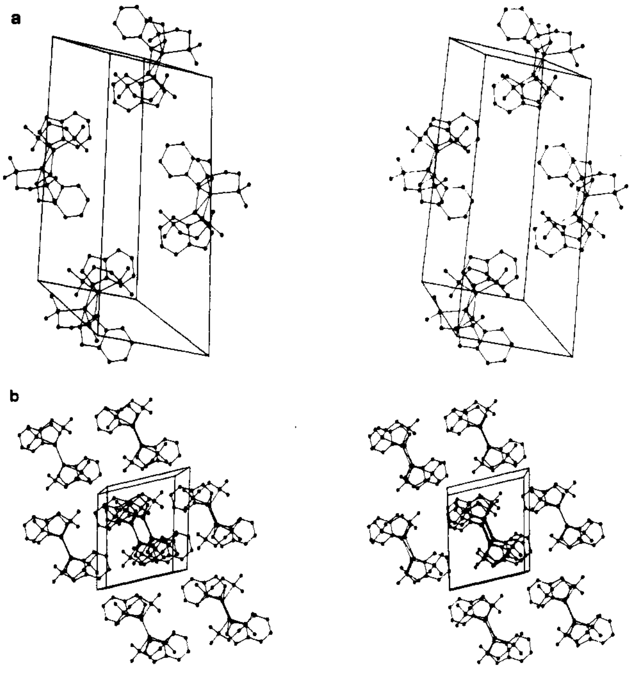

Figure 8. Stereoviews of crystal packing in [M–indole·TMEDA]$_2$; (a) M = Li; (b) M = Na.

Why are syn or anti isomers preferred? The packing plots of 1 and 2 (Figure 8) do not indicate that crystal effects may be important: there are no short intermolecular contacts between the dimer complexes. The ligand disorder in N-lithioindole·TMEDA might be a reason for the preference of the syn dimer in the crystal. The temperature factors of C(14) and C(15) show that the corresponding TMEDA methyl groups have space for thermal flexibility. The N(2)–Li–N(3) angle is 84.9°. In the Na species, this angle is smaller (76.7°). This leaves no space for thermal motion. Although MNDO calculations cannot be expected to be definitive, the results do give a general description of the situation. The energies calculated for the syn and anti isomers are identical. This finding is

---

(33) Bauer, W.; Schleyer, P. v. R. *Magn. Reson. Chem.* **1988**, *26*, 827.

supported by the NMR results. The 3:1 equilibrium of the two dimeric species shows that there is no large energetic preference in solution. The trans dimer of the PMDTA chelate of sodioindole shows that metal–donor contacts are preferred over intramolecular metal–carbon bonding. The tridentate donor satisfies the coordination sphere of the Na^+ cation and reduces the σ and π character even of the Na–N bonds.

Experimental Section

All manipulations were carried out under an argon atmosphere by using standard Schlenk techniques. All solvents were destilled from Na/K alloy under argon. Sodium *tert*-amylate was prepared by reaction of NaH with *tert*-amyl alkohol under reflux for 6 h.

[^{7}Li]Lithioindole·TMEDA (1): Indole (874 mg, 7.47 mmol) was dissolved in 20 mL of benzene and 1.4 mL of TMEDA (9.33 mmol). BuLi/hexane (4.7 mL, 7.52 mmol) was added, and the mixture was stored at room temperature for 2 h. Hexane (20 mL) was added, and the slightly red colored solution was stored at 0 °C. After 1 day colorless crystals of X-ray quality had formed, yield 1.56 g (58.8%).

[^{6}Li]Lithioindole·TMEDA: The reaction was carried out as described for 1 by using labeled *n*-Bu^{6}Li, yield 205 mg, (28.9%).

Sodioindole·TMEDA (2): (a) Preparation from indole, TMEDA, *n*-BuLi and sodium *tert*-amylate: The reaction was carried out as described for 1, using 2 mmol of indole, TMEDA, and *n*-BuLi each. Sodium *tert*-amylate in hexane (2.5 mL, 2.7 mmol) was added, and after 2 days at 0 °C colorless crystals had formed, yield 259 mg (35.5%). (b) Preparation from indole, TMEDA and *n*-BuNa:[34] *n*-BuNa (1200 mg, 15 mmol) was dissolved by addition of a solution of freshly distilled TMEDA (2.5 mL, 16.5 mmol) in 60 mL of *n*-hexane. A solution of indole (1650 mg, 14 mmol) in 20 mL of benzene was added slowly, whereupon the product precipitated from a red solution. The solid was filtered off, washed several times with *n*-hexane, and dried, yield 2.10 g (56%). Another 200 mg was obtained from the filtrate upon concentration and cooling.

Sodioindole·PMDTA (3): Preparation from indole, PMDTA, and *n*-BuNa: A suspension of *n*-BuNa (650 mg, 8 mmol) in 50 mL of hexane was added slowly to a solution of indole (900 mg, 7.7 mmol) in 30 mL of benzene. Stirring was continued for 30 min. Upon addition of PMDTA (1.9 mL, 9 mmol) most of the precipitate dissolved. The filtrate, cooled to 7 °C, yielded colourless crystals of **3** (2.30 g, 94%).

Suitable crystals of **1**, **2**, and **3**, obtained through slow crystallization from benzene/hexane (1:1), were sealed into capillaries under argon and mounted on the diffractometer. Initial investigations revealed the crystal systems to be monoclinic, triclinic, and monoclinic, respectively. Final lattice parameters were determined from least-squares refinement of the angular settings of 18 strong, accurately centered reflections. The data were corrected for crystal decay and Lorentz and polarization effects and converted into structure factors. No absorption correction was applied. The TMEDA–ligand in **1** is severely disordered. Atom C(13) was refined isotropically in two positions (C(13a), C(13b)) with site occupation factors 0.436 and 0.564, respectively. Additional data pertinent to the crystal structure determination are summarized in Table VII.

NMR measurements were carried out on a JEOL GX400 spectrometer (9.4 T). A selective 5-mm ^{1}H probehead (ROESY), a dual 5-mm ^{13}C, ^{1}H probehead (^{13}C), and a 10-mm multinuclear probehead (^{6}Li, ^{1}H HOESY) were used. Selected spectral parameters were as follows: ROESY (Figure 4): spectral width 671 Hz (f_1, f_2); 90° pulse width 35 μs (attenuated), data matrix size 1024 (t_2) × 128 (t_1) points, zero filling in t_1 to 256 points, exponential line broadening (BF 0.1) in both dimensions, mixing time 150 ms; 64 scans per t_1 increment. ^{13}C spectra: spectral width 25 000 Hz, 32K points, 90° pulse width 9 μs, relaxation delay 4.2 s, exponential line broadening (BF 1.5). ^{6}Li,^{1}H HOESY (Figure 7): spectral width 800 Hz (f_2) and 3790 Hz ($f_1 = {}^1$H), data matrix size 512 (t_2) × 128 (t_1) points, zero filling in t_1 to 256 points; 16 scans per t_1 increment; exponential line broadening in t_2, Gaussian window in t_1; mixing time 1.8 s; ^{6}Li spectra are referenced to 1 M LiBr in THF/THF-d_8; no corrections for bulk susceptibilities are made.

Acknowledgment. We thank Dr. R. Snaith (Cambridge) for interesting discussions. This work was supported by the Deutsche Forschungsgemeinschaft, the Fonds der chemischen Industrie, the Volkswagen Stiftung, and the Convex Computer Corp.

Supplementary Material Available: Listings of crystal data, thermal parameters, bond distances and angles, and hydrogen atom coordinates (10 pages); listings of observed and calculated structure factors (27 pages). Ordering information is given on any current masthead page.

---

[34] Bauer, W.; Pi, R.; Brix, B.; Schade, C.; Schleyer, P. v. R. *J. Organomet. Chem.* **1986**, *306*, 61.